23

Studying Ion Channel Dysfunction and Arrythmogenesis in the Human Atrium: A Computational Approach

Sanjay R. Kharche, Phillip R. Law, and Henggui Zhang
The University of Manchester, Manchester, UK

1. Introduction

Human atrial fibrillation (AF) is the most common sustained clinically observed cardiac arrhythmia causing mortality and morbidity in patients with increasing incidence in the elderly (Aronow 2009; Wetzel, Hindricks et al. 2009). It is prevalent in the developed world and a considerable burden on health care services in the UK and elsewhere (Stewart, Murphy et al. 2004; Aronow 2008a; Aronow 2008b). AF is a heterogeneously occurring disease often in complex with embolic stroke, thromboembolism, heart failure and other conditions (Novo, Mansueto et al. 2008; Bourke and Boyle 2009; Roy, Talajic et al. 2009). The treatment of paroxysmal AF includes pharmacological intervention primarily targeting cellular ion channel function (Ehrlich and Nattel 2009; Viswanathan and Page 2009). Persistent AF where episodes last for prolonged periods possibly requires electrical cardioversion (Wijffels and Crijns 2003; Conway, Musco et al. 2009) or repeated surgical interventions that isolate focal trigger sites that induce AF (Gaita, Riccardi et al. 2002; Saltman and Gillinov 2009; Stabile, Bertaglia et al. 2009). A better understanding of the underlying ion channel and structural mechanisms of AF will assist in design of improved clinical therapy at all stages of the disease.

The structure of the human atrium is shown in Fig. 1. Mechanisms underlying the genesis of AF are poorly understood yet. It is believed to be predominantly initiated by focal ectopic activity in the cristae terminalis of the right atrium, and pulmonary vein ostia in the left atrium (Haissaguerre, Jais et al. 1998). Spontaneous focal activities in the atrium could also be generated by intracellular calcium ($[Ca^{2+}]_i$) dysfunction (Chou and Chen 2009). The ectopic activity, under AF conditions, normally leads to a persistent single mother rotor of re-entrant excitation circuits. Upon interaction with anatomical obstacles along with intra-atrial electrical heterogeneity, the mother rotor wavefront breaks giving rise to smaller randomly propagating electrical wavefronts resulting in rapid erratic excitation of the atria (Moe, Rheinboldt et al. 1964) leading to uncoordinated contractions of the myocardium, which is reflected in the abnormal P-wave and R-R intervals of clinical ECG (Rosso and Kistler 2009). Recently a new mechanism, "AF begets AF" (Wijffels, Kirchhof et al. 1995) due to *AF induced electrical remodelling* (AFER), has been identified by which rapid excitation of atrial tissue gives rise to persistent AF AFER produces remarkable reduction in atrial *action potential (AP) duration* (APD) and effective refractive period (ERP), which are associated with

AF-induced changes in electrophysiology of ion channels. Several experimental studies have studied the effects of AFER on individual ion channels of human atrial myocytes (Bosch, Zeng et al. 1999; Workman, Kane et al. 2001; Bosch and Nattel 2002; Balana, Dobrev et al. 2003; Ravens and Cerbai 2008), and have identified several ion channels remodelled by chronic AF (Bosch, Zeng et al. 1999; Workman, Kane et al. 2001) .

Another mechanism underlying the genesis of AF is ion channel dysfunction arising from genetic mutations. There is growing interest in identifying genetic bases underlying familial AF following the first study by Chen et al. (Chen, Xu et al. 2003). In the rare but debilitating cases of familial AF, or lone AF, there is no apparent structural remodelling that precludes the onset of AF. However, several clinical studies have characterised the familial nature of several genetic defects that lead to AF (Chen, Xu et al. 2003; Xia, Jin et al. 2005; Makiyama, Akao et al. 2008; Restier, Cheng et al. 2008; Zhang, Yin et al. 2008; Li, Huang et al. 2009; Yang, Li et al. 2009). Hormonal imbalance during AF also causes electrical remodelling (Cai, Gong et al. 2007; Cai, Shan et al. 2009) that facilitates AF, but is not considered in this Chapter.

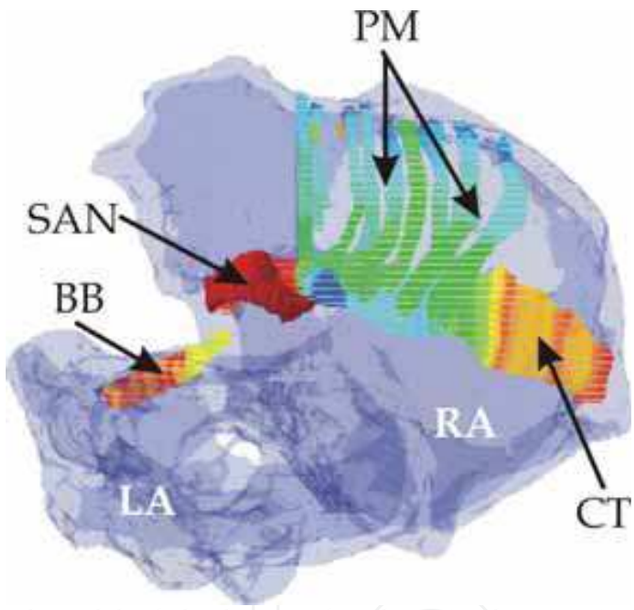

Fig. 1. 3D anatomical model of the human female atria showing internal structure and conduction pathways (figure adapted from our previous study (Zhang, Garratt et al. 2009)). Atrial tissue in the left (LA) and right (RA) atria is homogeneous (translucent blue). The sino-atrial node (SAN) is the pacemaker wherefrom cardiac electrical excitations originate. The main atrial conduction pathways, *i.e.* pectinate muscles (PM), cristae terminalis (CT) and the Bachman's bundles (BB), are the tissue types which possess electrical and structural heterogeneity and contribute to a small proportion of total atrial mass.

Experimental and clinical electrophysiological studies are vital to improve our understanding of AF and its underlying mechanisms. Such studies, however, require vast resources and involve ethical considerations. In addition, the effects of cellular level electrophysiological remodelling at multi-scale levels of cellular and spatially extended tissues is practically impossible in a clinical or physiology laboratory environment. Recently powerful biophysically detailed mathematical models of cardiac cells (Courtemanche,

Ramirez et al. 1998; Nygren, Fiset et al. 1998; Zhang, Holden et al. 2000; Pandit, Clark et al. 2001; ten Tusscher, Noble et al. 2004) and spatially extended tissues have been developed. Such biophysically detailed models of cardiac cells and tissues offer cost effective alternatives to experimental studies to investigate and dissect the effects changes in individual ion channels on cellular AP (Zhang, Garratt et al. 2005; Zhang, Zhao et al. 2007; Salle, Kharche et al. 2008) and tissue conduction properties (Kharche, Garratt et al. 2008; Kharche and Zhang 2008; Keldermann, ten Tusscher et al. 2009). With the ready availability of vast computational power, simulation offers an excellent complimentary method of studying AF *in silico* (Kharche, Seemann et al. 2008; Reumann, Fitch et al. 2008; Bordas, Carpentieri et al. 2009).

In this Chapter, we present a review of some of our recent works on studies of AFER and gene mutations in genesis and maintenance of AF. Comprehensive computational techniques for the quantification of the effects of AFER at cellular and tissue levels are described. Our simulation data at a multi-scale tissue level supported the "AF begets AF" hypothesis (Zhang, Garratt et al. 2005; Kharche, Seemann et al. 2007; Kharche, Seemann et al. 2008; Kharche and Zhang 2008), and demonstrated the dramatic pro-fibrillatory effects of Kir2.1 V93I gene mutation on the human atrium computational study (Kharche, Garratt et al. 2008). Techniques of high performance computing and visualisation of the computationally intensive 3D simulations are discussed.

2. Multi-scale simulation of the effects of AFER and Ione AF

In our studies of human atrial AF, we choose the widely used biophysically detailed cell model for human atrial AP developed by Courtemanche *et al.* (Courtemanche, Ramirez et al. 1998) (CRN). This 21 variable electrophysiological model consists of several sarcolemmal ion channel currents, pumps and exchanger currents, along with a sufficiently detailed intracellular ionic homeostasis mechanism. The model is able to reproduce human atrial AP accurately. Electrophysiological changes due to AFER and Kir2.1 V93I gene mutation can be immediately incorporated into this model allowing ready simulation of the resulting AP and $[Ca^{2+}]_i$ transients. Further, as described later in this section, the cellular models can be incorporated into multi-cellular tissue models using reaction diffusion formulations to simulate conduction propagation behaviour. To quantify the effects of AFER and Kir2.1 V93I gene mutation, a series of experimental protocols are computationally emulated quantifying their effects on atrial excitation at cellular and 3D anatomically detailed models.

2.1 Single cell modelling: electrophysiological changes due to AFER and monogenic AF

AFER and Kir2.1 V93I mutation both alter the biophysical properties of sarcolemmal ion channels underlying human atrial AP. Changes in ion channel current densities, time kinetics and steady state properties of ion channels have been quantified by experimental and clinical studies. The experimental data regarding AFER was obtained from two extensive studies wherein the effects of chronic human AF on atrial ion channels properties were studied. The study by Bosch et al. (Bosch, Zeng et al. 1999) considered patients with AF episodes lasting for more then 1 month (AF1), while the study by Workman et al. (Workman, Kane et al. 2001) considers patients with AF episodes lasting for more than 6 months (Workman, Kane et al. 2001) (AF2). In brief, remodelling in AF1 includes a 235% increase of the maximal conductance of the inward rectifier potassium current I_{K1}, 74%

reduction of the conductance of the L-type calcium current $I_{Ca,L}$, 85% reduction of conductance of the transient outward current (I_{to}), a shift of -16 mV of the I_{to} steady-state activation, and a -1.6 mV shift of sodium current (I_{Na}) steady state activation. Fast inactivation kinetics of $I_{Ca,L}$ is slowed down, and was implemented as a 62% increase of the voltage dependent inactivation time constant. Remodelling in AF2 includes a 90% increase of I_{K1}, 64% reduction of $I_{Ca,L}$, 65% reduction of I_{to}, 12% increase of the sustained outward potassium current (I_{Ksus}), and a 12% reduction of the sodium potassium pump ($I_{Na,K}$). Both AF1 and AF2 data have been incorporated into the CRN model in our previous study (Zhang, Garratt et al. 2005).

Simulation of Kir2.1 V93I gene mutation was based on the recent clinical data from Xia et al. (Xia, Jin et al. 2005) who examined several generations of a large family with hereditary AF associated with Kir2.1 V93I gene mutation. The Kir2.1 gene primarily regulates the I_{K1} channel current, which is modelled as

$$I_{K1} = g_{K1}(V - E_K) \tag{1}$$

$$g_{K1} = ag_{K1\max} + \frac{(1-a)g_{K1\max}}{1 + e^{(b(V-c))}} \tag{2}$$

where V is the cell membrane potential; E_K the reversal potential of the channel; g_{K1max} the maximal channel conductance; "a" is the fraction of the channel conductance that is voltage-independent, (1-a) is the fraction of the channel conductance that is voltage-dependent, "b" the steepness of the g_{K1}-V relationship; "c" is the half point of the g_{K1}-V relationship. In simulations, we considered different conditions of the mutation from Control (Con), to heterozygous (Het) to homozygous (Hom) cases. Parametric values of equations 1 and 2 for different conditions of Kir2.1 V93I gene mutation are listed in Table 1, which were based on the experimental study of Xia et al. (Xia, Jin et al., 2005).

Experimental data sets of AFER and Kir2.1 V93I gene mutation as described above were then incorporated into the CRN human atrial AP model to simulate their effects on human atrial excitation at cellular and tissue models. A quantitative summary of all results is given in Table 2.

2.2 Quantifying the effects of AFER and Kir2.1 V93I gene mutation on atrial APs at cellular level

We first quantify the functional effects of AFER and Kir2.1 V93I mutation on atrial cellular APs. Excitable models, including human atrial cell models, are usually at resting state far away from the oscillating state and show rate dependent adaptation upon periodic pacing, similar to those seen experimentally (Workman, Kane et al. 2001; Cherry, Hastings et al. 2008). Therefore, the models have to be conditioned with several pulses before stable excitations can be elicited. In case of the CRN model, it was found that 10 pulses at a pacing cycle length (PCL) of 1 s was sufficient conditioning. Upon simulation, characteristics of AP profiles were quantified by measuring the resting potential and APD at 90% repolarisation (APD_{90}), the overshoot and the maximal upstroke velocity, dV/dt_{max}. APD_{90} reflects the overall changes in ion channel function during AP. dV/dt_{max} on the other hand, not only

Quantity	Con	Het	Hom
g_{K1max} (nS/pF)	0.09 (100%)	0.13 (141% ↑)	0.16 (173% ↑)
a	0.0	0.0355	0.0575
b (mV^{-1})	0.070	0.156	0.232
c (mV)	-80.0	-60.1	-54.7

Table 1. Parameters of I_{K1} equations (1-2) for various Kir2.1 V93I gene mutation conditions. Values were determined based on experimental data of Xia et al. (Xia, Jin et al. 2005) under Con, Het and Hom conditions.

influences cellular behaviour, but also the conduction properties at tissue level (Biktashev 2002). Due to the large increase in repolarisation potassium currents and reduction in depolarising currents, the AP profiles show large abbreviation in APD_{90} under AFER and Kir2.1 V93I gene mutation conditions. APD abbreviation under AFER conditions is due to a integral actions of remodelled ion channels. However, in the gene mutation condition, such an abbreviation is caused by gain-in-function of the I_{K1} channel. The effects of AFER and Kir2.1 V93I gene mutation on AP profiles are shown in Fig. 2.

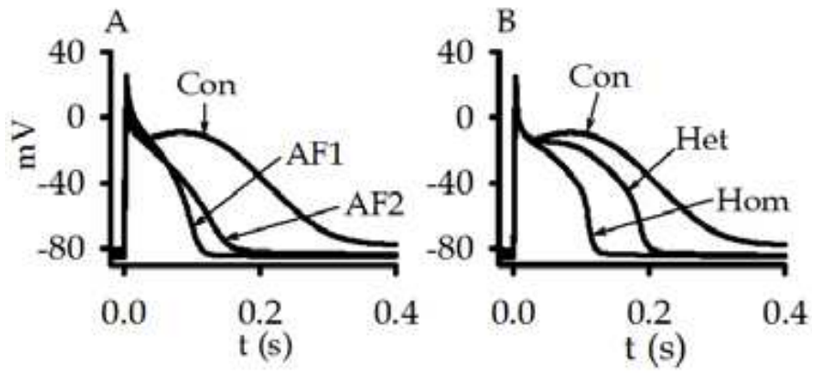

Fig. 2. AP profiles under AFER (A) and Kir2.1 V93I gene mutation (B) conditions. AFER and the mutation cause a dramatic abbreviation of APD.

APD restitution (APDr) measures the excitation behaviour of atrial cells subjected to premature pulses immediately after a previous excitation (Franz, Karasik et al. 1997; Qi, Tang et al. 1997; Kim, Kim et al. 2002; Burashnikov and Antzelevitch 2005; Cherry, Hastings et al. 2008). Recent experimental and modelling studies have shown the correlation between the maximal slope of APDr greater than unity and instability of re-entrant excitation waves in 2D and 3D tissues (Xie, Qu et al. 2002; Banville, Chattipakorn et al. 2004; ten Tusscher, Mourad et al. 2009). In our study, APDr is computed using a standard S1S2 protocol. A train of ten conditioning stimuli (S1) at a physiological PCL were applied before the premature pulse (S2) was applied. The time interval between the final conditioning excitation and onset of the premature excitation emulates atrial diastolic interval (DI), or the time the atrial organ has for recovery from the previous excitation. In the CRN model, S1 and S2 have stimulus amplitude of 2 nA and duration of 2 ms. A plot of the DI against APD_{90} gives APDr, as shown in Fig. 3 for Control, AFER and Kir2.1 V93I gene mutation conditions. At large DI,

APDr curves have negligible slopes and show AP profiles under physiological rates of pacing. At low DI, however, the slopes are noticeable. Under AFER conditions, the computed APDr slopes under various conditions are much greater than under Control conditions (Table 2).

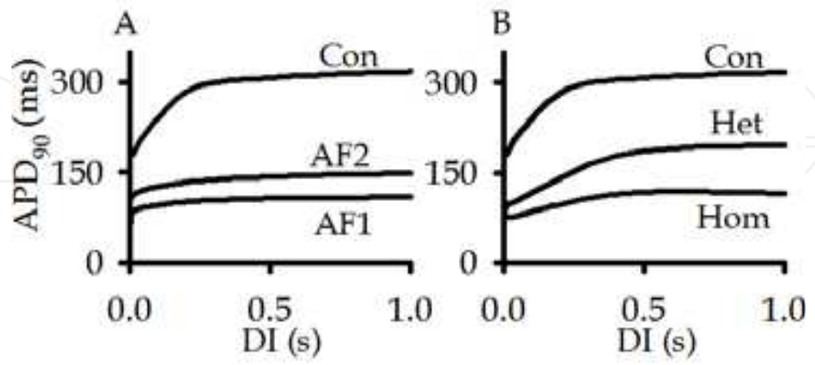

Fig. 3. APDr profiles under AFER (A) and Kir2.1 V93I gene mutation (B) conditions. At large DI, APDr curves reflect the changes in APD_{90} under Control (Con) and AF (AF1, AF2, Het and Hom) conditions. At low DI, the maximal slopes of APDr curves indicate the instabilities in 2D and 3D simulations. Quantitative details are given in Table 2.

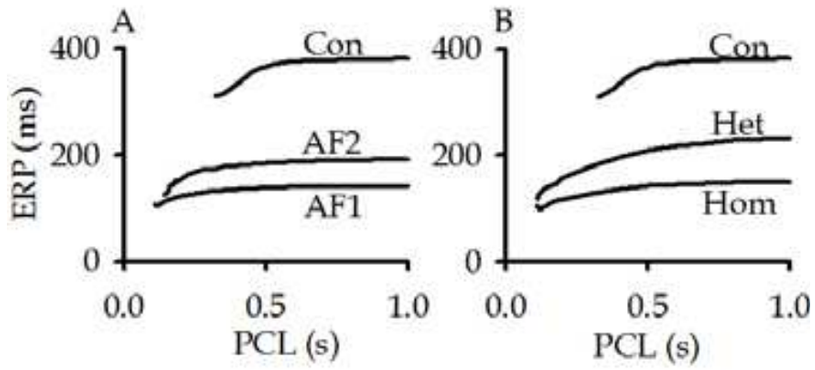

Fig. 4. ERP restitution curves under AFER (A) and Kir2.1 V93I gene mutation (B) conditions.

Shortening of atrial APD and effective refractory period (ERP) are well recognised features of atrial electrical activities during AF. ERP is generally measured by using cellular or tissue preparations (Workman, Kane et al. 2001; Laurent, Moe et al. 2008). In our studies, we adopted the cell based experimental protocol as described by Workman et al. (Workman, Kane et al. 2001) where the cell was stimulated 10 times at various PCLs. A premature stimulus S2 was then applied. The maximal time interval between S1 and S2 where the final excitation has AP amplitude of 80% as compared to the premature pulses is defined as the ERP. Due to the rate dependent adaptability of atrial AP, we usually compute ERP at several PCL values to obtain an ERP restitution curve. Results are shown in Fig. 4. It can be seen that AF reduces ERP (Table 2). Such a reduction is in qualitative agreement with experimental observations and clinical data (Workman, Kane et al. 2001; Li, Hertervig et al. 2002; Oliveira, da Silva et al. 2007).

2.3 1D and 2D tissue modelling

Human atrial tissue is spatially and electrically homogeneous tissue (Jalife 2003; Seemann, Hoper et al. 2006). The primary sources of heterogeneity in the human atrium are the conduction pathways as shown in Fig. 1, which contribute only a small fraction to total atrial mass. Therefore, it is reasonable to take human atrial tissue as homogeneous in simulations of the effects of AFER and Kir2.1 V93I gene mutation on atrial excitations (Kharche, Garratt et al. 2008; Kharche, Seemann et al. 2008).

To simulate atrial excitation at the tissue level, the CRN atrial cell AP model is incorporated into tissue models using a mono-domain reaction diffusion partial differential equation,

$$\frac{\partial V(r)}{\partial t} = -D\nabla^2 V(r) + I_{ion}(r) \tag{3}$$

where D is the homogeneous diffusion constant mimicking the intracellular gap junctional coupling, ∇^2 is the Laplacian operator and I_{ion} is the total reactive current at any given spatial location r in the tissue associated with the ion channels of the atrial cell at r. We take D to be 0.03125 mm^2/ms to give physiological value of conduction velocity (CV) of 0.265 mm/ms, which falls in the range of physiological measurements. Such a formulation is sufficient for our purposes as we do not consider any extracellular potentials, fluids or indeed mechanical activity, for which more complex bi-domain formulations have to be adopted (Potse, Dube et al. 2006; Whiteley 2007; Vigmond, Weber dos Santos et al. 2008; Linge, Sundnes et al. 2009; Morgan, Plank et al. 2009).

To quantify the functional effects of AFER and Kir2.1 V93I gene mutation on atrial CV restitution (CVr) and temporal vulnerability (VW), models of 1D homogeneous atrial strand were used. CVr is computed by conditioning the 1D strand (S1) after which a premature pulse is applied. The CV of the second propagation as a function of the inter-pulse duration, or PCL, is termed as CVr. CV of propagations is computed from the central region of the strands as shown in Fig 5A. CVr for AFER and the gene mutation conditions are shown in Fig. 5, B and C, where the stimulation protocol is also illustrated. As can be seen, AF reduces solitary wave CV, i.e. CV at large PCL, or low pacing rates. Such CV reduction is not due to any changes in the inter-cellular coupling in the tissue, but solely due to the changes of atrial cell AP profiles. Our simulation data revealed that atrial tissue has better ability to sustain atrial conduction at fast pacing rates under AFER or gene mutation conditions than under Control conditions.

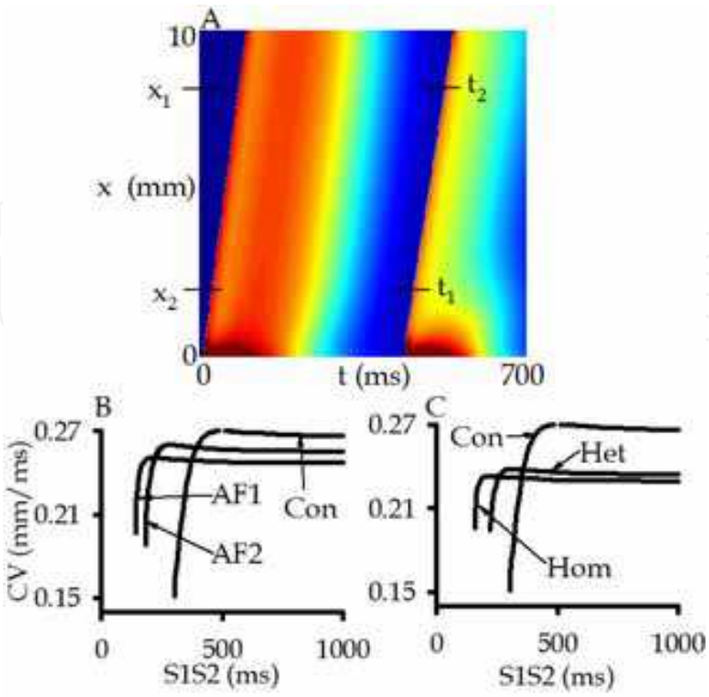

Fig. 5. (A) Electrical waves in a 1D strand where the first wave conditions the tissue, whilst the second wave is initiated after an interval S2. CV is computed according to when the second wave is at x1 (t1) and x2 (t2). (B) CVr under AFER conditions. (C) CVr under Kir2.1 V93I gene mutation conditions.

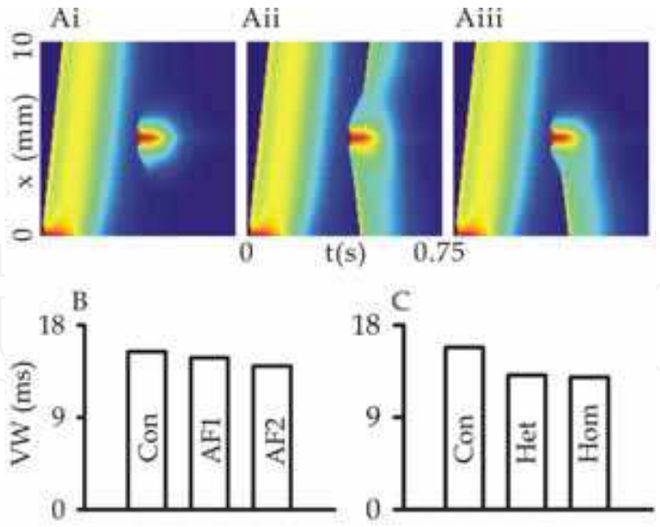

Fig. 6. Atrial excitation wave evoked by a S2 stimulus, applied at a time delay after the conditioning excitation wave, can be either bi-directional blocked (Ai) if the time delay is too soon, or bi-directional conduction (Aii) if the time delay is too late, or uni-directional conduction block (Aiii) if the time delay falls in the VW. Computed VW under AFER conditions (B) and Kir2.1 V93I gene mutation conditions (C).

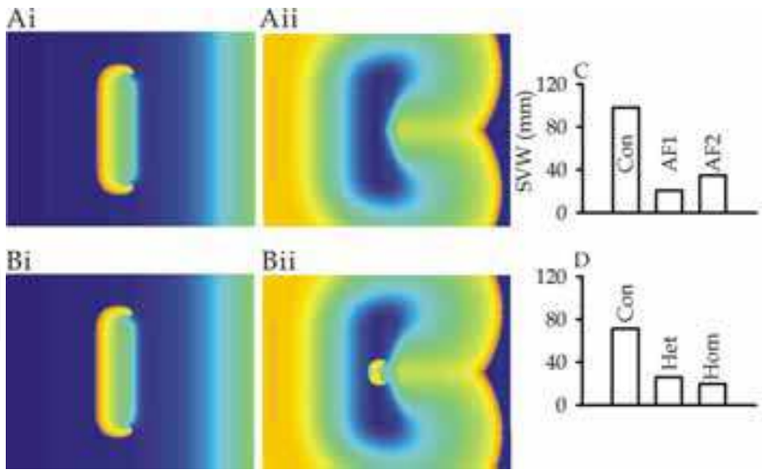

Fig. 7. Computed SVW from 2D tissue models by applying a premature stimulus in the repolarisation tail of a conditioning pulse so as to evoke a figure of 8 re-entry (Ai, Aii and Bi, Bii). The minimal length of the premature stimulus such that the evoked reentry sustains is termed as SVW. (C) SVW under AFER conditions. (D) SVW under Kir2.1 V93I gene mutation conditions. AFER and the gene mutation cause a dramatic reduction of SVW allowing the tissue to sustain re-entry with reduced substrate size.

Uni-directional conduction block in atria can lead to genesis of re-entrant excitation waves. Temporal vulnerability or vulnerability window (VW) measures the vulnerability of cardiac tissue to genesis of uni-directional conduction block. VW is computed by allowing a single solitary wave to propagate from one end of the 1D tissue to the other. After certain duration and in the repolarisation phase in the middle of the tissue, a premature pulse is applied. The time window during which the premature pulse elicits uni-directional propagation block is termed as the VW. Fig. 6 illustrates the protocol and also shows the measured VW under AFER and Kir2.1 V93I gene mutation conditions.

The effects of AFER and the Kir2.1 gene mutation on atrial tissue's spatial vulnerability are quantified by using 2D homogeneous models of human atrial tissue. Spatial vulnerability (SVW) is computed as the minimal atrial substrate size that can sustain re-entrant waves. To this end, a sufficiently long pulse as shown in Fig. 7 is applied in the repolarisation tail of the conditioning pulse, giving rise to a figure of "8" re-entrant waves. The minimum length that sustains such re-entry is termed as SVW. The results for AFER and gene mutation conditions are given in Fig. 7.

Effects of the AFER and Kir2.1 V93I gene mutation on the dynamical behaviours of re-entrant excitation waves are also studied. In 2D tissues, re-entrant wave simulations are performed in a tissue with a size of 37.5 cm x 37.5 cm. In simulations, re-entrant waves are initiated by using a cross-field stimulation protocol. After allowing a planar wave to sufficiently propagate through the 2D sheet, a cross-field stimulus is applied so as to initiate re-entry (Kharche, Seemann et al. 2007). Upon initiation of a re-entrant wave in the middle of the tissue, the re-entrant waves are allowed to evolve for several seconds. Results are shown in Fig. 8. Under Control conditions, the 2D re-entrant waves self-terminate. However, under AFER and Kir2.1 V93I gene mutation conditions, re-entrant waves become persistent. During the simulation, time series of APs from representative locations were also

recorded to allow analysis of dominant frequency of the re-entry. It is shown that the rates of atrial re-entrant excitation waves increased markedly from Control conditions to AF ER and gene mutation conditions. Traced trajectory of the core tips of re-entrant excitation illustrated the increased stability and persistence of the re-entrant waves under AFER and gene mutation conditions. These results are shown in Fig. 9.

2.4 Simulation of re-entrant waves in a 3D realistic geometry

The 3D anatomically detailed spatial model of human female atria as shown in Fig. 1 was developed in a previous study (Seemann, Hoper et al. 2006). It is based on the anatomical geometry of the human atria reconstructed from the visible human project (Ackerman, 1991; Ackerman and Banvard 2000). The anatomical model consists of electrically homogeneous atrial tissue, the SAN and conduction pathways. The SAN is the main pacemaker wherefrom cardiac electrical excitation originates. The conduction pathways are electrically and structurally heterogeneous and assist in normal conduction of electrical excitation in the human atrium. In our studies, we however study re-entrant waves and therefore do not consider SAN electrical activity, nor the heterogeneity associated with the conduction pathways. All cells in our 3D anatomical model simulations are considered to be electrically homogeneous.

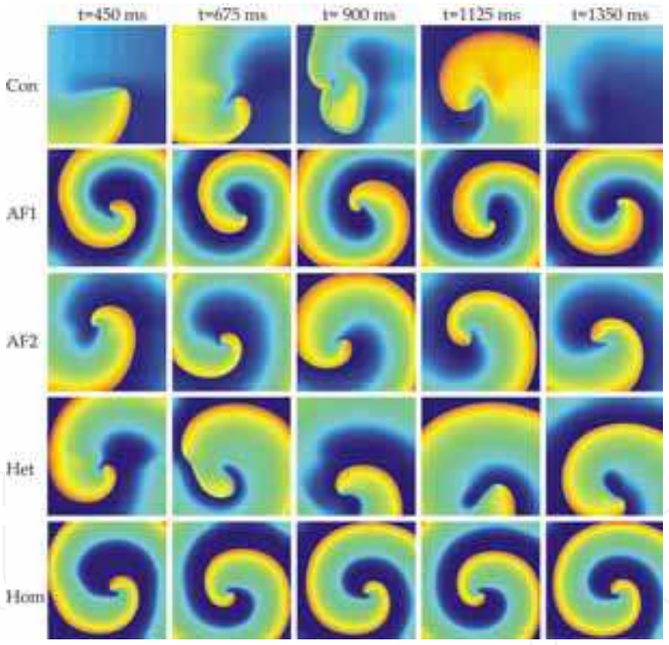

Fig. 8. Representative frames at regular intervals from 2D homogeneous re-entrant waves simulations under Control, AFER and Kri2.1 V93I gene mutation conditions. Re-entry self-terminates under Control conditions (top row), but becomes persistent under AFER and gene mutation conditions.

Re-entrant waves were initiated and allowed to propagate through the electrically and anatomically homogeneous model under Control, AFER and gene mutation conditions. The re-entrant waves were initiated using a protocol similar to the 2D case at a place in the right atrium to reduce boundary effects and interference from anatomical obstacles. The right

atrium was chosen to be ideal as it offers minimal anatomical defects interfering with the initial evolution of the re-entrant waves. Results from the 3D simulations under Control and AFER and gene mutation conditions are shown in Fig. 10.

Under Control conditions, re-entry self-terminated at around 4.2 s. AFER however rendered re-entry to be persistent. Again, if we study representative AP profiles during the simulation, we can see that AF increases the dominant frequency. The dominant frequency of oscillations in Control case is low at less than 3 Hz. In contrast, under AFER conditions, the re-entry is persistent with rapid excitation rate. AFER increases stability of the mother rotor under AF2 conditions. Due to the anatomical defects, the mother rotor degenerates into smaller persistent erratic propagating wavelets, with a dominant frequency more than 10 Hz. Similar results were obtained under the Kir2.1 V93I gene mutation conditions as shown in Fig. 11.

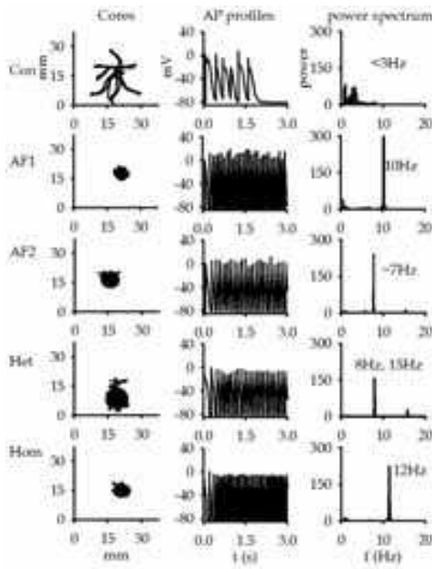

Fig. 9. Dynamical behaviours of 2D re-entrant waves as shown in Fig. 8 with core tip traces (left column), representative AP profiles (middle column) and dominant frequency of the AP profiles (right column) under various AFER and gene mutation conditions. Re-entrant waves are more stable and cause high rate of atrial tissue excitation under AFER and gene mutation conditions.

Our simulations have also shown another important mechanism by which re-entry becomes persistent without effects of AFER or gene mutation. Upon initiation of re-entry close to a blood vessel ostium, the electrical wave readily becomes anchored, as seen in Fig. 12. Such anchoring of an electrical propagation also gives rise to persistent and rapid excitation of atrial tissue.

2.5 Numerical considerations, algorithms and visualisation

Time integration of the CRN cellular models was carried out at a constant time step of 0.005 ms as given in the original CRN model. In the spatial 1D and 2D models, a space step of 0.1 mm was used in an explicit central Euler spatial integration scheme. The inter-node distance

of 0.1 mm represents human atrial size which is close to physiological values. In the 3D models, the space step was taken to be 0.33 mm, which allowed use of a time step of 0.5 ms. These choices gave stable solutions independent of integration parameters.
The 2D and 3D spatial models are large with 140625 and more than 26 x 10^6 nodes respectively. Parallelisation is therefore an important part of cardiac simulations. Solvers that used shared memory parallelism (OpenMP) and large distributed memory parallelism (MPI) were developed in our laboratory. Scaling of the solvers is shown in Fig. 13. In addition to parallelisation, novel cardiac specific algorithms that exploit peculiarities of the model were developed (Kharche, Seemann et al. 2008). The full geometrical model demands very large amounts of contiguous memory. 3D Atrial tissue geometry occupies about 8% geometry of the total data set, due to atrium being thin walled with large holes of atrial chambers and vena caves. We re-structured the computer code such that only atrial nodes, *i.e.* only 8% of the total 26 million nodes and related information are stored in the computer memory. This improved efficacy of memory usage. By re-numbering the real atrial nodes we are not storing any data points that are not atrium. The memory required is reduced to less than 10 GB in the 3D case, and the required computer floating point operations (flops) are also reduced.

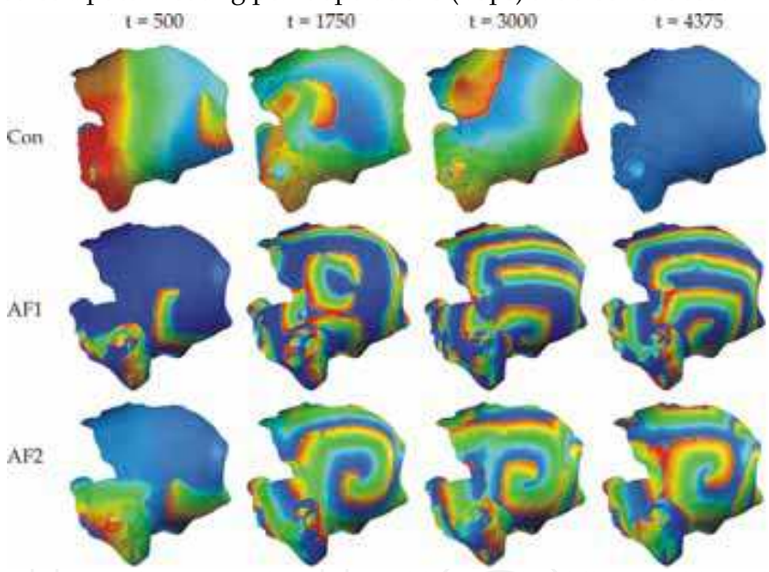

Fig. 10. 3D re-entry under Control (top panels), AF1 (middle panels) and AF2 (bottom panels). Re-entry self-terminates under Control conditions in 4.2 s. Under AF1 conditions, the narrow wavelength re-entrant wave breaks up due to interaction with anatomical obstacles and gives rise to rapid erratic electrical propagations which are persistent. AF2 caused the re-entrant rotor to be stable and gave rise to a mother rotor.

The 3D simulations produce large data sets of more than 30 GB. Traditionally this output is then post-processed to obtain measures quantifying the simulation, e.g. scroll wave filament meander, and to visualise the dynamics of the electrical propagations. Each output file consists of a binary data file of approximately 150 MB size. Efficient visualisation of the 3D data shown in Figs. 10 and 12 was carried using the RAVE package (Grimstead, Kharche et al. 2007) developed elsewhere. We have also developed visualisation techniques based on the visualisation package Advanced Visualisation System (AVS) developed by Manchester Visualisation Centre. This is versatile high level graphical software with a high level of

functionality. Images in Fig. 11 were produced using diamond shaped glyphs, each of which was colour coded with a scalar value, namely the value of voltage at that location.
For smaller visualisation jobs, *e.g.* 2D visualisation, we have used MATLAB due to its functionality and transparent scripting. Development of visualisation scripts using MATLAB is relatively straightforward with a high level of functionality. MATLAB is also available to our laboratory locally. Having successfully developed 2D visualisation pipelines using MATLAB, AVS as a high level visual programming environment is also versatile and the results obtained using MATLAB can be replicated by AVS.

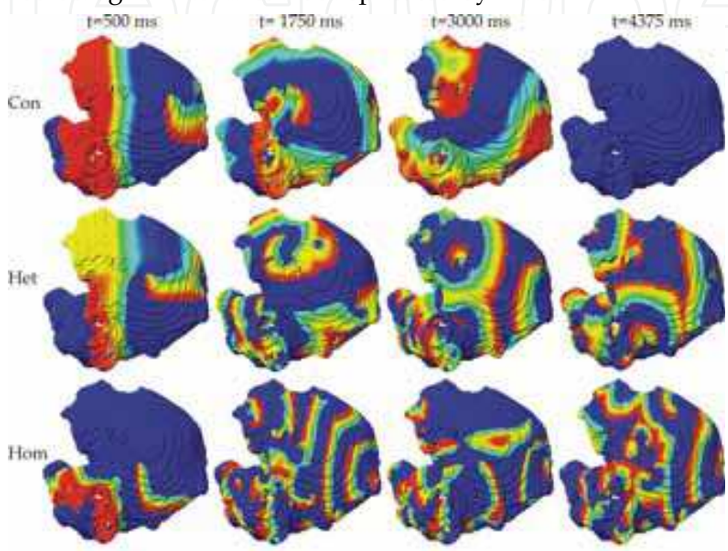

Fig. 11. 3D re-entry under Control (top panels), various Kir2.1 V93I gene mutation conditions (Het, middle panels; Hom, bottom panels). With Kri2.1 V93I gene mutation, condition, the re-entry became erratic leading to rapid excitation of atrial tissue.

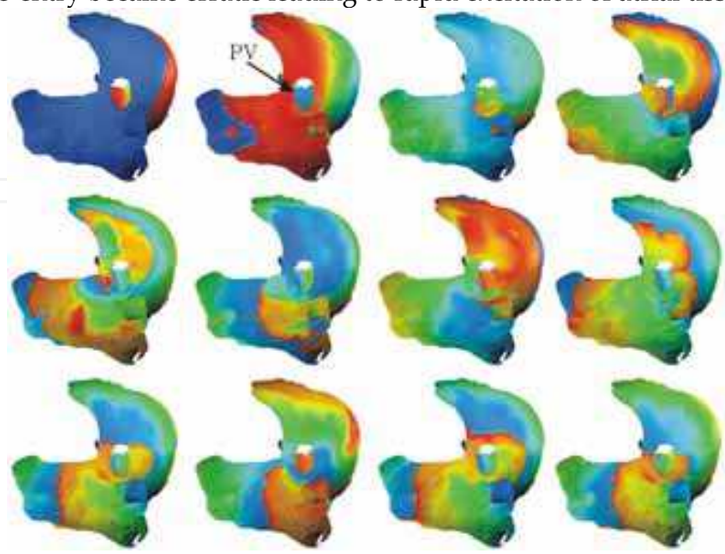

Fig. 12. Anchoring of re-entrant wave to pulmonary vein (PV). Location of PV is marked by the arrow in the first panel of the second column.

Model	Quantity	Con	AF1	AF2	Het	Hom
Cell	Resting potential (mV)	-80.5	-85.2	-83.8	-84.59	-85.07
	APD_{90} (ms)	313.0	108.5	147.6	196.2	137.2
	Overshoot (mV)	22.9	24.6	25.0	24.3	24.1
	dV/dt_{max} (mV/ms)	147.2	86.5	97.2	113.4	98.1
	APDr maximal slope	0.91	4.63	1.56	2.2	0.46
	ERP (ms) (stimulus interval ~ 1 s)	318.0	142.0	192.0	232.0	150.0
1D	CV (mm/ms)	0.27	0.25	0.26	0.26	0.25
	VW (ms)	15.4	14.8	14	13.1	12.9
	Wavelength (mm)	84.51	27.13	38.22	67.3	56.5
2D	LS (s)	1.8	> 10	> 10	>10	>10
	DF (Hz)	<3.0	10.0	7.0	8-15	12
	Tip meander area (mm^2)	615.0	48.0	72.0	101.2	76.1
	SVW (mm)	99.1	20.5	34.7	26.2	17.0
3D	LS (s)	4.2	> 6	> 6	>6	>6
	DF (Hz)	3.0	6.7	6.1	10.2	13.5

Table 2. Quantitative summary of the effects of AFER and Kir2.1 V93I gene mutation on atrial excitations.

3. Conclusions and future work

Our simulation results have shown that both the AFER and Kir2.1 V93I mutation shortened atrial APD and increased the maximal slopes of APDr. They reduced atrial ERP and the intra-atrial CV, all of which facilitated high rate atrial excitation and conduction as observe d experimentally and clinically in AF patients. Due to the large increase in repolarisation currents, the both the AFER and Kir2.1 V93I gene mutation reduced tissue's temporal VW. However, they also reduced the minimal substrate size required to sustain re-entry. Collectively of all these suggested the pro-arrhythmic effects of AFER and Kir2.1 gene mutation. Our results also showed AFER and the gene mutation increased the stability of re-entry, leading them to be persistent.

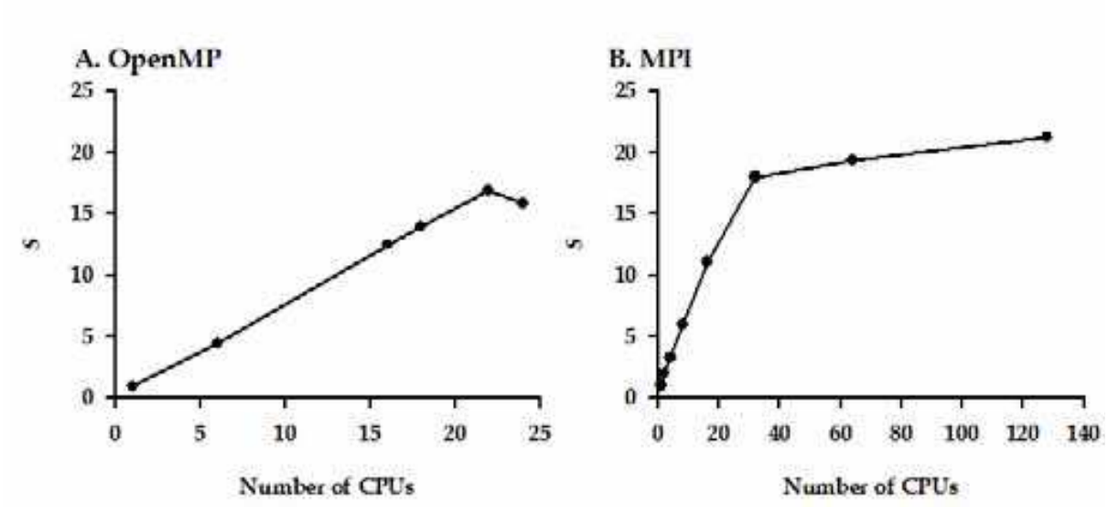

Fig. 13. (A) Scaling of the shared memory (OpenMP) solver. (B) Scaling of the distributed memory (MPI) solver.

These data have provided the first evidence in support of the hypothesis of "AF begetting AF". The methods described above characterise several aspects of the AFER and Kir2.1 gene mutation on generating and sustaining AF. Future studies may consider mechanism involving malfunctioning of intracellular $[Ca^{2+}]_i$ handling (Hove-Madsen, Prat-Vidal et al. 2006), spontaneous firing at atrial blood vessel ostia, interaction between SAN and atria. In addition to macro re-entrant waves, micro re-entry is also an important factor responsible for AF (Markowitz, Nemirovksy et al. 2007). Inclusion of the electrical and spatial heterogeneities in the various tissue sub-types in the atrium will further our understanding the genesis of AF, especially the micro-entry due to heterogeneity boundaries. Computational methods and algorithms can be further improved. This is especially relevant for patient specific simulations where real time results are vital. An immediate aspect of the current simulation-visualisation pipeline that can be addressed is that of incorporating the visualisation, at least partly, into the simulation process. This will enormously improve efficacy of the 3D simulations.

4. References

Aronow, W. S. (2008a). "Management of atrial fibrillation--Part 1." Compr Ther **34**(3-4): 126-33.

Aronow, W. S. (2008b). "Management of atrial fibrillation--Part 2." Compr Ther **34**(3-4): 134-42.

Aronow, W. S. (2009). "Management of atrial fibrillation in the elderly." Minerva Med **100**(1): 3-24.

Balana, B., D. Dobrev, et al. (2003). "Decreased ATP-sensitive K(+) current density during chronic human atrial fibrillation." J Mol Cell Cardiol **35**(12): 1399-405.

Banville, I., N. Chattipakorn, et al. (2004). "Restitution dynamics during pacing and arrhythmias in isolated pig hearts." J Cardiovasc Electrophysiol **15**(4): 455-63.

Biktashev, V. N. (2002). "Dissipation of the excitation wave fronts." Phys Rev Lett **89**(16): 168102.

Bordas, R., B. Carpentieri, et al. (2009). "Simulation of cardiac electrophysiology on next-generation high-performance computers." Philos Transact A Math Phys Eng Sci **367**(1895): 1951-69.

Bosch, R. F. and S. Nattel (2002). "Cellular electrophysiology of atrial fibrillation." Cardiovasc Res **54**(2): 259-69.

Bosch, R. F., X. Zeng, et al. (1999). "Ionic mechanisms of electrical remodeling in human atrial fibrillation." Cardiovasc Res **44**(1): 121-31.

Bourke, T. and N. G. Boyle (2009). "Atrial fibrillation and congestive heart failure." Minerva Med **100**(2): 137-43.

Burashnikov, A. and C. Antzelevitch (2005). "Role of repolarization restitution in the development of coarse and fine atrial fibrillation in the isolated canine right atria." J Cardiovasc Electrophysiol **16**(6): 639-45.

Cai, B., L. Shan, et al. (2009). "Homocysteine modulates sodium channel currents in human atrial myocytes." Toxicology **256**(3): 201-6.

Cai, B. Z., D. M. Gong, et al. (2007). "Homocysteine inhibits potassium channels in human atrial myocytes." Clin Exp Pharmacol Physiol **34**(9): 851-5.

Chen, Y. H., S. J. Xu, et al. (2003). "KCNQ1 gain-of-function mutation in familial atrial fibrillation." Science **299**(5604): 251-4.

Cherry, E. M., H. M. Hastings, et al. (2008). "Dynamics of human atrial cell models: restitution, memory, and intracellular calcium dynamics in single cells." Prog Biophys Mol Biol **98**(1): 24-37.

Chou, C. C. and P. S. Chen (2009). "New concepts in atrial fibrillation: neural mechanisms and calcium dynamics." Cardiol Clin **27**(1): 35-43, viii.

Conway, E. L., S. Musco, et al. (2009). "Drug therapy for atrial fibrillation." Cardiol Clin **27**(1): 109-23, ix.

Courtemanche, M., R. J. Ramirez, et al. (1998). "Ionic mechanisms underlying human atrial action potential properties: insights from a mathematical model." Am J Physiol **275**(1 Pt 2): H301-21.

Ehrlich, J. R. and S. Nattel (2009). "Novel approaches for pharmacological management of atrial fibrillation." Drugs **69**(7): 757-74.

Franz, M. R., P. L. Karasik, et al. (1997). "Electrical remodeling of the human atrium: similar effects in patients with chronic atrial fibrillation and atrial flutter." J Am Coll Cardiol **30**(7): 1785-92.

Gaita, F., R. Riccardi, et al. (2002). "Surgical approaches to atrial fibrillation." Card Electrophysiol Rev **6**(4): 401-5.

Grimstead, I. J., S. Kharche, et al. (2007). Viewing 0.3Tb Heart Simulation Data At Your Desk. EG UK Theory and Practice of Computer Graphics D. D. Ik Soo Lim.

Haissaguerre, M., P. Jais, et al. (1998). "Spontaneous initiation of atrial fibrillation by ectopic beats originating in the pulmonary veins." N Engl J Med **339**(10): 659-66.

Hove-Madsen, L., C. Prat-Vidal, et al. (2006). "Adenosine A2A receptors are expressed in human atrial myocytes and modulate spontaneous sarcoplasmic reticulum calcium release." Cardiovasc Res **72**(2): 292-302.

Jalife, J. (2003). "Experimental and clinical AF mechanisms: bridging the divide." J Interv Card Electrophysiol **9**(2): 85-92.

Keldermann, R. H., K. H. ten Tusscher, et al. (2009). "A computational study of mother rotor VF in the human ventricles." Am J Physiol Heart Circ Physiol **296**(2): H370-9.

Kharche, S., C. J. Garratt, et al. (2008). "Atrial proarrhythmia due to increased inward rectifier current (I(K1)) arising from KCNJ2 mutation--a simulation study." Prog Biophys Mol Biol **98**(2-3): 186-97.

Kharche, S., G. Seemann, et al. (2007). Scroll Waves in 3D Virtual Human Atria: A Computational Study. LNCS. F. B. S. a. G. Seemann. **4466:** 129–138.

Kharche, S., G. Seemann, et al. (2008). "Simulation of clinical electrophysiology in 3D human atria: a high-performance computing and high-performance visualization application." Concurrency and Computation: Practice and Experience **20**(11): 10.

Kharche, S. and H. Zhang (2008). "Simulating the effects of atrial fibrillation induced electrical remodeling: a comprehensive simulation study." Conf Proc IEEE Eng Med Biol Soc **2008**: 593-6.

Kim, B. S., Y. H. Kim, et al. (2002). "Action potential duration restitution kinetics in human atrial fibrillation." J Am Coll Cardiol **39**(8): 1329-36.

Laurent, G., G. Moe, et al. (2008). "Experimental studies of atrial fibrillation: a comparison of two pacing models." Am J Physiol Heart Circ Physiol **294**(3): H1206-15.

Li, Q., H. Huang, et al. (2009). "Gain-of-function mutation of Nav1.5 in atrial fibrillation enhances cellular excitability and lowers the threshold for action potential firing." Biochem Biophys Res Commun **380**(1): 132-7.

Li, Z., E. Hertervig, et al. (2002). "Dispersion of refractoriness in patients with paroxysmal atrial fibrillation. Evaluation with simultaneous endocardial recordings from both atria." J Electrocardiol **35**(3): 227-34.

Linge, S., J. Sundnes, et al. (2009). "Numerical solution of the bidomain equations." Philos Transact A Math Phys Eng Sci **367**(1895): 1931-50.

Makiyama, T., M. Akao, et al. (2008). "A novel SCN5A gain-of-function mutation M1875T associated with familial atrial fibrillation." J Am Coll Cardiol **52**(16): 1326-34.

Markowitz, S. M., D. Nemirovksy, et al. (2007). "Adenosine-insensitive focal atrial tachycardia: evidence for de novo micro-re-entry in the human atrium." J Am Coll Cardiol **49**(12): 1324-33.

Moe, G. K., W. C. Rheinboldt, et al. (1964). "A Computer Model of Atrial Fibrillation." Am Heart J **67**: 200-20.

Morgan, S. W., G. Plank, et al. (2009). "Low energy defibrillation in human cardiac tissue: a simulation study." Biophys J **96**(4): 1364-73.

Novo, G., P. Mansueto, et al. (2008). "Risk factors, atrial fibrillation and thromboembolic events." Int Angiol **27**(5): 433-8.

Nygren, A., C. Fiset, et al. (1998). "Mathematical model of an adult human atrial cell: the role of K+ currents in repolarization." Circ Res **82**(1): 63-81.

Oliveira, M. M., N. da Silva, et al. (2007). "Enhanced dispersion of atrial refractoriness as an electrophysiological substrate for vulnerability to atrial fibrillation in patients with paroxysmal atrial fibrillation." Rev Port Cardiol **26**(7-8): 691-702.

Pandit, S. V., R. B. Clark, et al. (2001). "A mathematical model of action potential heterogeneity in adult rat left ventricular myocytes." Biophys J **81**(6): 3029-51.

Potse, M., B. Dube, et al. (2006). "A comparison of monodomain and bidomain reaction-diffusion models for action potential propagation in the human heart." IEEE Trans Biomed Eng **53**(12 Pt 1): 2425-35.

Qi, A., C. Tang, et al. (1997). "Characteristics of restitution kinetics in repolarization of rabbit atrium." Can J Physiol Pharmacol **75**(4): 255-62.

Ravens, U. and E. Cerbai (2008). "Role of potassium currents in cardiac arrhythmias." Europace **10**(10): 1133-7.

Restier, L., L. Cheng, et al. (2008). "Mechanisms by which atrial fibrillation-associated mutations in the S1 domain of KCNQ1 slow deactivation of IKs channels." J Physiol **586**(Pt 17): 4179-91.

Reumann, M., B. G. Fitch, et al. (2008). "Large scale cardiac modeling on the Blue Gene supercomputer." Conf Proc IEEE Eng Med Biol Soc **2008**: 577-80.

Rosso, R. and P. Kistler (2009). "Focal atrial tachycardia." Heart.

Roy, D., M. Talajic, et al. (2009). "Atrial fibrillation and congestive heart failure." Curr Opin Cardiol **24**(1): 29-34.

Salle, L., S. Kharche, et al. (2008). "Mechanisms underlying adaptation of action potential duration by pacing rate in rat myocytes." Prog Biophys Mol Biol **96**(1-3): 305-20.

Saltman, A. E. and A. M. Gillinov (2009). "Surgical approaches for atrial fibrillation." Cardiol Clin **27**(1): 179-88, x.

Seemann, G., C. Hoper, et al. (2006). "Heterogeneous three-dimensional anatomical and electrophysiological model of human atria." Philos Transact A Math Phys Eng Sci **364**(1843): 1465-81.

Stabile, G., E. Bertaglia, et al. (2009). "Role of pulmonary veins isolation in persistent atrial fibrillation ablation: the pulmonary vein isolation in persistent atrial fibrillation (PIPA) study." Pacing Clin Electrophysiol **32 Suppl 1**: S116-9.

Stewart, S., N. F. Murphy, et al. (2004). "Cost of an emerging epidemic: an economic analysis of atrial fibrillation in the UK." Heart **90**(3): 286-92.

ten Tusscher, K. H., A. Mourad, et al. (2009). "Organization of ventricular fibrillation in the human heart: experiments and models." Exp Physiol **94**(5): 553-62.

ten Tusscher, K. H., D. Noble, et al. (2004). "A model for human ventricular tissue." Am J Physiol Heart Circ Physiol **286**(4): H1573-89.

Vigmond, E. J., R. Weber dos Santos, et al. (2008). "Solvers for the cardiac bidomain equations." Prog Biophys Mol Biol **96**(1-3): 3-18.

Viswanathan, M. N. and R. L. Page (2009). "Pharmacological therapy for atrial fibrillation: current options and new agents." Expert Opin Investig Drugs **18**(4): 417-31.

Wetzel, U., G. Hindricks, et al. (2009). "Atrial fibrillation in the elderly." Minerva Med **100**(2): 145-50.

Whiteley, J. P. (2007). "Physiology driven adaptivity for the numerical solution of the bidomain equations." Ann Biomed Eng **35**(9): 1510-20.

Wijffels, M. C. and H. J. Crijns (2003). "Recent advances in drug therapy for atrial fibrillation." J Cardiovasc Electrophysiol **14**(9 Suppl): S40-7.

Wijffels, M. C., C. J. Kirchhof, et al. (1995). "Atrial fibrillation begets atrial fibrillation. A study in awake chronically instrumented goats." Circulation **92**(7): 1954-68.

Workman, A. J., K. A. Kane, et al. (2001). "The contribution of ionic currents to changes in refractoriness of human atrial myocytes associated with chronic atrial fibrillation." Cardiovasc Res **52**(2): 226-35.

Xia, M., Q. Jin, et al. (2005). "A Kir2.1 gain-of-function mutation underlies familial atrial fibrillation." Biochem Biophys Res Commun **332**(4): 1012-9.

Xie, F., Z. Qu, et al. (2002). "Electrical refractory period restitution and spiral wave reentry in simulated cardiac tissue." Am J Physiol Heart Circ Physiol **283**(1): H448-60.

Yang, Y., J. Li, et al. (2009). "Novel KCNA5 loss-of-function mutations responsible for atrial fibrillation." J Hum Genet.

Zhang, H., C. J. Garratt, et al. (2009). "Remodelling of cellular excitation (reaction) and intercellular coupling (diffusion) by chronic atrial fibrillation represented by a reaction-diffusion system." Physica D: Nonlinear Phenomena **238**(11-12): 8.

Zhang, H., C. J. Garratt, et al. (2005). "Role of up-regulation of IK1 in action potential shortening associated with atrial fibrillation in humans." Cardiovasc Res **66**(3): 493-502.

Zhang, H., A. V. Holden, et al. (2000). "Mathematical models of action potentials in the periphery and center of the rabbit sinoatrial node." Am J Physiol Heart Circ Physiol **279**(1): H397-421.

Zhang, H., Y. Zhao, et al. (2007). "Computational evaluation of the roles of Na+ current, iNa, and cell death in cardiac pacemaking and driving." Am J Physiol Heart Circ Physiol **292**(1): H165-74.

Zhang, S., K. Yin, et al. (2008). "Identification of a novel KCNQ1 mutation associated with both Jervell and Lange-Nielsen and Romano-Ward forms of long QT syndrome in a Chinese family." BMC Med Genet **9**: 24.

IntechOpen

Recent Advances in Biomedical Engineering

Edited by Ganesh R Naik

ISBN 978-953-307-004-9
Hard cover, 660 pages
Publisher InTech
Published online 01, October, 2009
Published in print edition October, 2009

The field of biomedical engineering has expanded markedly in the past ten years. This growth is supported by advances in biological science, which have created new opportunities for development of tools for diagnosis and therapy for human disease. The discipline focuses both on development of new biomaterials, analytical methodologies and on the application of concepts drawn from engineering, computing, mathematics, chemical and physical sciences to advance biomedical knowledge while improving the effectiveness and delivery of clinical medicine. Biomedical engineering now encompasses a range of fields of specialization including bioinstrumentation, bioimaging, biomechanics, biomaterials, and biomolecular engineering. Biomedical engineering covers recent advances in the growing field of biomedical technology, instrumentation, and administration. Contributions focus on theoretical and practical problems associated with the development of medical technology; the introduction of new engineering methods into public health; hospitals and patient care; the improvement of diagnosis and therapy; and biomedical information storage and retrieval. The book is directed at engineering students in their final year of undergraduate studies or in their graduate studies. Most undergraduate students majoring in biomedical engineering are faced with a decision, early in their program of study, regarding the field in which they would like to specialize. Each chosen specialty has a specific set of course requirements and is supplemented by wise selection of elective and supporting coursework. Also, many young students of biomedical engineering use independent research projects as a source of inspiration and preparation but have difficulty identifying research areas that are right for them. Therefore, a second goal of this book is to link knowledge of basic science and engineering to fields of specialization and current research. The editor would like to thank the authors, who have committed so much effort to the publication of this work.

How to reference

In order to correctly reference this scholarly work, feel free to copy and paste the following:

Sanjay R. Kharche, Phillip R. Law and Henggui Zhang (2009). Studying Ion Channel Dysfunction and Arrythmogenesis in the Human Atrium: A Computational Approach, Recent Advances in Biomedical Engineering, Ganesh R Naik (Ed.), ISBN: 978-953-307-004-9, InTech, Available from: http://www.intechopen.com/books/recent-advances-in-biomedical-engineering/studying-ion-channel-dysfunction-and-arrythmogenesis-in-the-human-atrium-a-computational-approach

INTECH
open science | open minds

InTech Europe
University Campus STeP Ri

InTech China
Unit 405, Office Block, Hotel Equatorial Shanghai

www.intechopen.com

Slavka Krautzeka 83/A
51000 Rijeka, Croatia
Phone: +385 (51) 770 447
Fax: +385 (51) 686 166
www.intechopen.com

No.65, Yan An Road (West), Shanghai, 200040, China
中国上海市延安西路65号上海国际贵都大饭店办公楼405单元
Phone: +86-21-62489820
Fax: +86-21-62489821

IntechOpen

IntechOpen